SPATIAL ANALYSIS OF RAIN RATES FOR TROPICAL CYCLONES AFFECTING MADAGASCAR AND MOZAMBIQUE

457

Corene J. Matyas[1] *, Sarah VanSchoick[2]
[1]University of Florida, Gainesville, Florida; [2]Santa Fe College, Gainesville, Florida

1. INTRODUCTION

When tropical cyclones (TCs) affect Madagascar and Mozambique, they can cause floods that impact livelihoods in these economically disadvantaged countries (Reason and Keibel 2004; Reason 2007; Brown 2009; Matyas and Silva 2013; Silva et al. 2015; Arivelo and Lin 2016). Research has been conducted on the genesis and tracks of TCs in this region (Jury et al. 1999; Vitart et al. 2003; Hoskins and Hodges 2005; Chang-Seng and Jury 2010; Ash and Matyas 2012; Matyas 2015), and rainfall variability in general (Reason et al. 2005; Williams et al. 2007). To better understand the evolution of rainfall events, it is important to calculate the distance that the rain field of a TC extends away from its circulation center to determine where and when rainfall will be received.

Rain rates can vary widely across a TC. Lonfat et al.'s (2004) study of global TC rain rates utilizing data from the Tropical Rainfall Measuring Mission (TRMM) Microwave Imager revealed that the peak frequency of rain rates is 1 mm/hr. More intense TCs tend to produce higher rain rates that extend farther from the storm's circulation. Rain rates and the spatial pattern of rainfall produced by a TC can also be influenced by topography (Arivelo and Lin 2016). Madagascar features elevated terrain that rises to 2000+ m along its major axis (Fig. 1), which should influence rainfall production in TCs that make landfall here. Therefore, we hypothesize that 1 mm/hr rain rates will extend farther from the storm's center when TCs over the Southwest Indian Ocean or Mozambique Channel attain a higher intensity or when their forward quadrants interact with the Malagasy Mountains.

* *Corresponding author address:* Corene J. Matyas, Univ. of Florida, Dept. of Geography, Gainesville, FL 32611-7315; e-mail matyas@ufl.edu

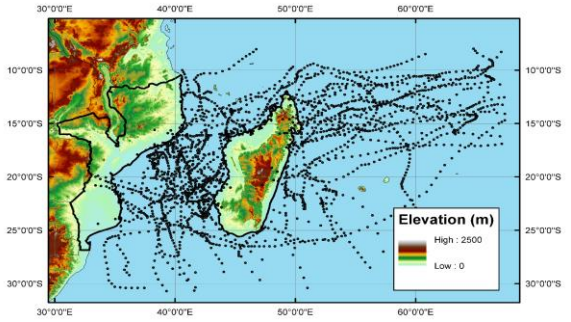

Fig. 1. Study region, elevation, and 3- hourly TC positions. Mozambique and Madagascar are outlined in black.

To test this hypothesis, we employ a Geographic Information System (GIS) to analyze rain rates every 3 hours from the TRMM 3B42 product for 38 TCs 1998-2015. After determining the extent of rainfall in each direction-relative quadrant, we investigate relationships with 1) storm location as a) interaction with topographical boundaries may lead to spatial clustering of high or low rainfall extents, and b) rain rates for TCs in the Mozambique Channel are lower than for other TCs (Chang et al. 2014), which could lead to a smaller extent, and 2) storm intensity as more intense TCs should have a larger extent of rainfall (Lonfat et al. 2004).

2. DATA AND METHODS

TC position and intensity data are taken from the IBTrACS dataset (Knapp et al. 2010). To match the TRMM temporal resolution, we linearly interpolate the 6-hr data to every 3 hours. We use the first column of data for WMO_Winds and only include observations when they are at least tropical depression intensity. We also eliminate from consideration observations that are not classified as tropical entities (e.g., subtropical, extratropically-

transitioned, too weak to have a recorded wind speed). To prevent four long-track storms from biasing the results, we limit the study region's longitudinal extent to 33° - 68° E.

We first convert the TRMM data to raster images. We then import them into a GIS and contour rates every 1 mm/hr (Fig. 2). After a sensitivity analysis utilizing rates of 1, 2, and 2.5 mm/hr, we discovered that using 1 mm/hr as the threshold to define the edge of the rain field produced the most reliable results across the TCs. In many cases, higher rain rates produced regions that were too small for analysis. Previous work by Lonfat et al. (2004) and Change et al. (2014) support this decision as rain rates for TCs globally peak near 1 mm/hr and rain rates for TCs in the SWIO are lower than those in other regions.

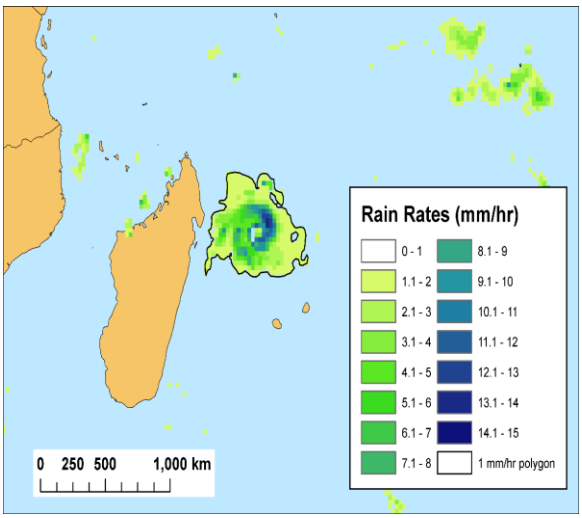

Fig. 2. Polygon defining the rain fields analyzed for Hudah (2000), with the perimeter corresponding to a rain rate of 1 mm/hr. Rainfall regions not outlined in black are not considered as their centroids extend more than 500 km from Hudah's center of circulation.

Next, we convert smoothed contours to polygons and determine the distance of each polygon's centroid from the TC's circulation center. We only include polygons with centroids <500 km from TC center (Jiang et al. 2011) to exclude rainfall produced from other weather systems (Fig. 2). In the final phase of the GIS analysis, we utilize a Python script to calculate the extent of rainfall. The script extends radial lines 750 km outward from the TC's center every 1° around the circle. At every location where a radial intersects with a polygon, the location of this intersection is recorded. The farthest intersection along each line is retained (Fig. 3). Then statistics are calculated for each quadrant, which are placed according to cardinal directions (NW, SW, SE, NE) (Guo and Matyas 2016). We calculate the average extent in each quadrant along with maximum, minimum, and standard deviation. In this study, we only report results of the average extent in each quadrant.

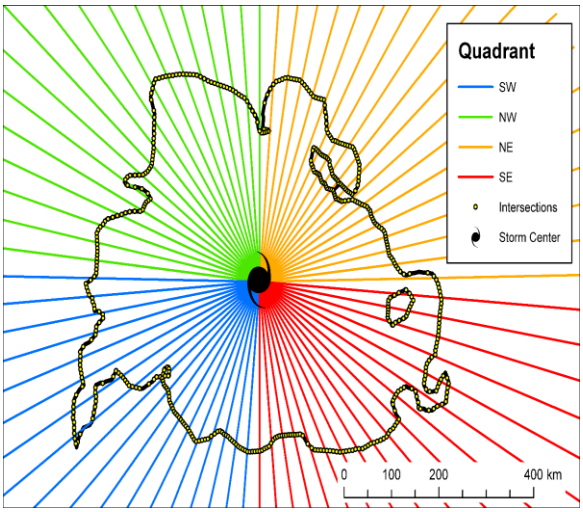

Fig. 3. Zoomed in view at same time as in Figure 2 showing extent lines (every 5° for display purposes) and polygon intersections every 1° divided into quadrants. The farthest intersecting point along each 1° line is used to calculate extent.

We add to our database at each observation time by examining the TC center's location and the location of the rain fields. We note whether the TC center is over the Southwest Indian Ocean (SWIO) or Mozambique Channel (MC). We perform an intersect operation with a shapefile of land areas to determine whether any part of the rain fields are over land. We include the maximum sustained wind speed, and also calculate the time since formation, since reaching maximum intensity, and since landfall. Negative values represent times before the event, while positive values are after the event.

3. STATISTICAL ANALYSIS

We hypothesize that rainfall extent may exhibit strong spatial patterns due to the influence of topography and/or the fact that many TCs reach their maximum intensity in the hours prior to their landfall over Madagascar.

Therefore, we check for spatial clustering of extent using Optimized Hot Spot Analysis in ArcMap. Statistically significant spatial clusters of high values (hot spots) and low values (cold spots) are identified by employing the Getis-Ord Gi* statistic (Ord and Getis 1995) which measures the intensity of clustering of high or low point values relative to neighboring points. In current study, the optimal fixed distance band is based on the average distance to 30 nearest neighbors. The null hypothesis is that the values associated with features are randomly distributed. The Getis-Ord Gi* statistic (Ord and Getis 1995) generates *z*- scores (standard deviations) and *p*- values (statistical probabilities) for each point feature. *Z*-scores farther from zero indicate more intense the clustering of values. The False Discovery Rate correction parameter is also applied to account for spatial dependence.

Three different statistical tests are employed to examine relationships between rainfall extent in each quadrant and storm location and intensity. We employ the Jonckheere-Terpstra (JT) Test for Ordered Alternatives and Spearman's Rank Correlation Analysis to test for relationships between intensity and rainfall extent in each quadrant. The JT test is performed by grouping observations into classes by increasing intensity: tropical depression, moderate tropical storm, severe tropical storm, tropical cyclone, and intensity tropical cyclone. We use Mann-Whitney *U* tests to examine differences in quadrant extent for rain fields over water vs. land and over the SWIO vs. MC.

4. RESULTS

Of the 38 TCs, 37% produce rainfall over land when they first form (Fig. 4a). Many are located over the MC or over land (Fig. 4b). Also, 70% of observations within the MC produce rainfall over land (Fig. 4c). The shortest span of the MC is 420 km, and average quadrant extents are 200 km, yielding a diameter of 400 km. Thus, chances are high that when a TC moves over the Channel, it will produce rainfall either over Madagascar or Mozambique. TCs approaching Madagascar from the northeast (Fig. 4c) are more typical examples of long-track storms where a TC intensifies while moving westward and makes landfall several days later. Most TCs produce their first rainfall over land when within 48 hours of landfall (Fig. 4d), but some large and/or slow-movers with looping tracks produce rainfall over land more than 4 days prior to landfall.

a)

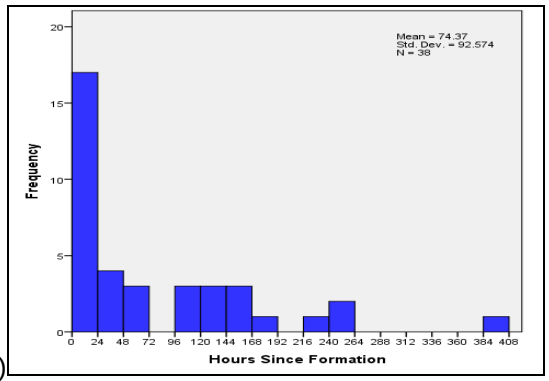

b)

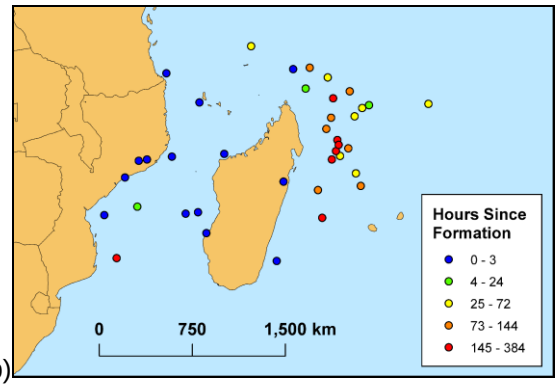

c)

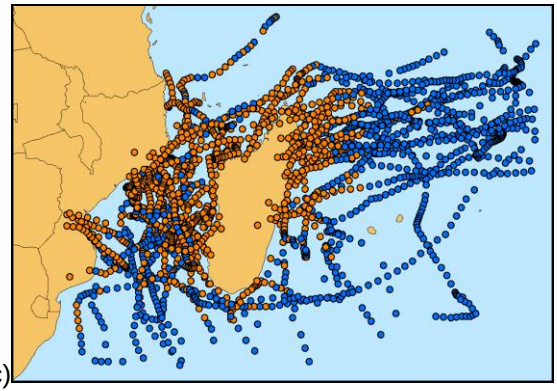

d)

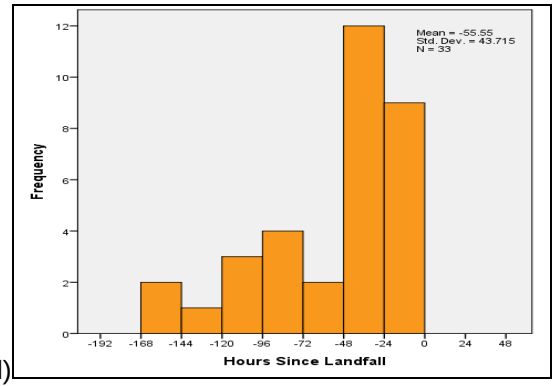

Fig. 4. a) Hours since formation and b) location of center when TC first produces rainfall over land. c) TC positions where rainfall occurs over land (orange) or not over land (blue), and d) time since landfall when rainfall first occurs over land (negative indicates time before landfall).

Whether the storm center is over the SWIO or MC and whether or not the rain fields intersect land make a difference in terms of rain field extent (Fig. 5). Rain fields are bigger over land and over the SWIO. Multiple Mann-Whitney *U* tests confirm the differences are statistically significant (p <0.02) for all quadrants save the NE for over-water locations. The western quadrants are the largest as TCs over the SWIO produce rain over Madagascar, and smallest for TCs producing rain over land when located over the MC, thus orography may aid rainfall development on the windward side and hinder it on the leeward side of Madagascar. The hot spot analysis examines this further.

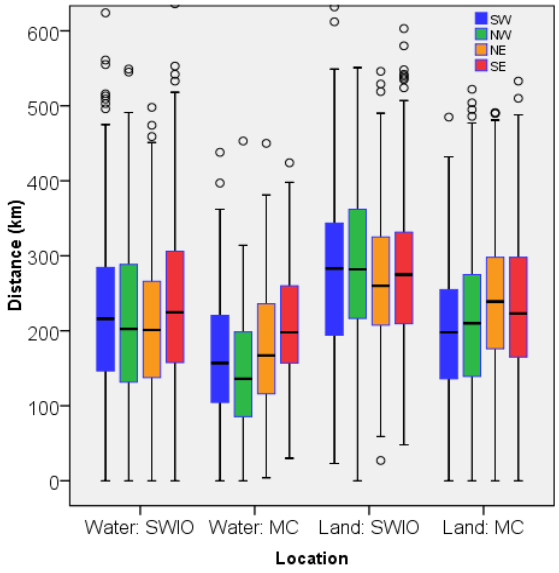

Fig. 5. Boxplot showing 25, 50, and 75th percentiles of rain field extent in each quadrant when the TC center is over different water bodies and whether or not rainfall is occurring over land.

The hot spot analysis shows that rain fields have large extents in all quadrants (Fig. 6a-d) as they approach Madagascar, especially on the leading western side. While orography may play a role, this region also features higher maximum sustained winds (Fig. 6e). However, higher wind speeds occur in the southern MC and the western side is smaller west of Madagascar, suggesting that winds off of the leeward side of the terrain may limit rainfall extent. The NE quadrant is large for TCs over parts of the MC where intensity is also lower. The SE quadrant has the weakest spatial clustering of TC extent (Table 1). This might be attributed to storm motion as it is the left rear quadrant for many TCs, but the left front quadrant for others where wind speeds are highest. The proximity to a deep tropical moisture source may explain why extents are larger in the northern (equatorward) part of the study region.

a)

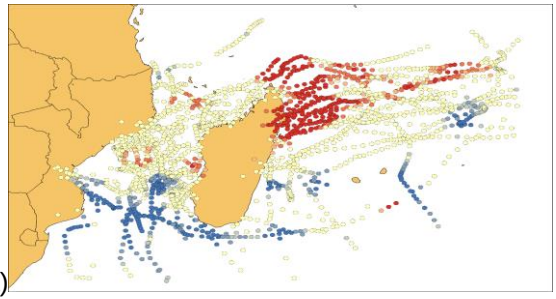

b)

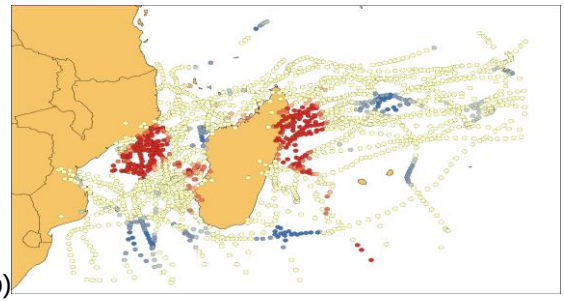

c)

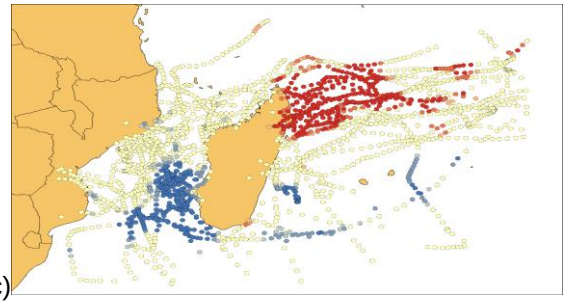

d)

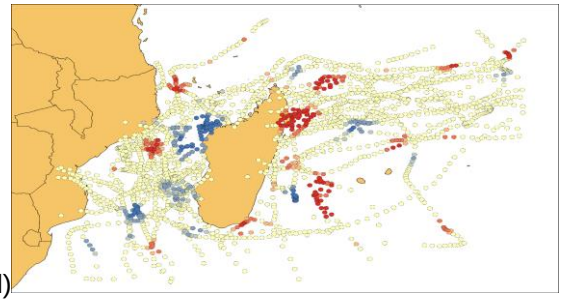

e)

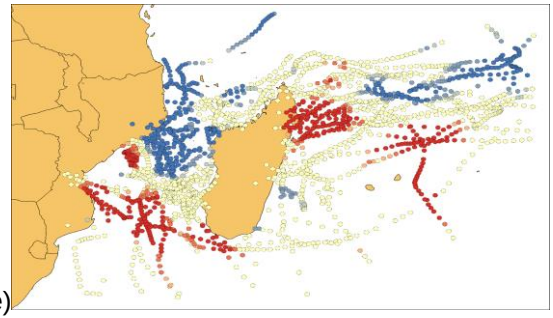

f)

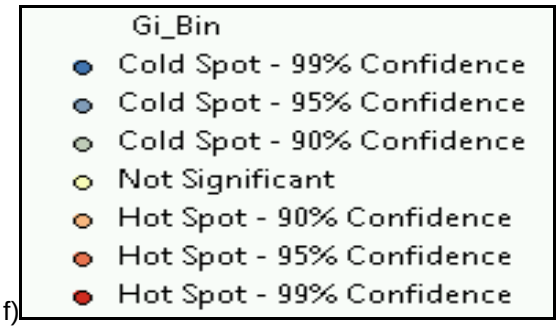

Fig. 6. Results of hot spot analysis for rainfall extent in a) NW, b) NE, c) SW, and d) SE quadrants, e) for maximum sustained wind speed. f) legend showing that clusters of higher (lower) values are hot (cold) spots.

Table 1. Statistics produced during hot spot analysis.

Quadrant	n	Mean Extent (km)	Avg. Dist. 30 Nearest Neighbors (km)	n Sig. Features
Northwest	2074	224	152	852
Southwest	2174	213	152	852
Southeast	2227	233	223	293
Northeast	2176	226	173	657

Results of the Jonckheere-Terpstra test (Table 2) confirm that extent increases with each class of intensity. Correlations of V_{max} with rain field extent are significant with 99% confidence (Table 2). The northwest quadrant exhibits the strongest correlation with intensity. In most cases, the northwest quadrant overlapped with the right front quadrant, however the strongest winds should be found in the left front quadrant for these TCs as they are in the Southern Hemisphere.

Table 2. Results of Jonckheere-Terpstra test results (tropical depression, moderate tropical storm, severe tropical storm, tropical cyclone, intense tropical cyclone) and Spearman's Rank correlation coefficients with maximum sustained wind speed each quadrant.

Quadrant	Jonckheere-Terpstra *p*-value	Vmax ρ
Northwest	<0.01	0.45
Southwest	<0.01	0.38
Southeast	<0.01	0.25
Northeast	<0.01	0.32

5. CONCLUSIONS AND FUTURE WORK

This study utilized satellite-based estimates of rain rates to define the spatial extent of TC rain fields over the SWIO and MC. Rain fields were defined using a GIS to contour the 1 mm/hr rain rate, and polygons with centroids located within 500 km of the centers of the 38 TCs were included in the analysis. The extent of rainfall was measured in each quadrant and the quadrant-averaged values were examined over space and in terms of storm intensity and location.

Results revealed strong spatial patterns in the extent of TC rain fields for storms over the SWIO and MC. More than a third of storms produced rainfall over land as they formed, and most of these were over the MC, explaining why rainfall extent for MC storms producing rainfall over land had smaller extent of 1 mm/hr rain rates when compared to TCs over the SWIO, as these systems were more intense as they produced rainfall over Madagascar. The smallest extents overall belonged to TCs over the MC that were not producing rainfall over land.

The hot spot analysis revealed strong spatial patterns in rain field extent for southwest, northwest, and northeast quadrants. Rain fields were large as TCs approached Madagascar. This result may be related to 1) storm intensity which is also high here, and/or 2) interaction with mountains where upslope flow ahead of the storm increased rainfall production. The western sides had smaller extents when located offshore west of Madagascar and this could be attributed to downslope flow from the mountains. Statistical tests revealed a statistically significant relationship between storm intensity and rainfall extent in all quadrants.

Future work will investigate TCs individually to better document potential topographic interactions. Data pertaining to moisture in the environment surrounding the storm will be examined to determine its relationship with rainfall extent as previous research has found that a connection to a source of deep tropical moisture helps to maintain rainfall production (Matyas 2017; Takakura et al. 2017), and storm size (Hill and Lackmann 2009) and rain fields (Zhou and Matyas 2018) tend to be larger when moisture is higher. We will also examine relationships between rainfall extent and vertical wind shear and storm motion, as these factors are known to produce asymmetries in storm structure. We will examine the difference between the largest and smallest quadrant to better quantify asymmetry.

6. ACKNOWLEDGEMENTS

This research was funded by the National Science Foundation's IUSE (Improving Undergraduate STEM Education) Pathways into Geoscience Program (ICER 1540729 and 1540724).

7. REFERENCES

Arivelo, T. A., and Y.-L. Lin, 2016: Climatology of Heavy Orographic Rainfall Induced by Tropical Cyclones over Madagascar: From Synoptic to Mesoscale Perspectives. *Earth Science Research*, **5,** 146.

Ash, K. D., and C. J. Matyas, 2012: The influences of ENSO and the Subtropical Indian Ocean Dipole on tropical cyclone trajectories in the South Indian Ocean. *Int. J. Climatol.*, **32,** 41-56.

Brown, M. L., Ed., 2009: *Madagascar's cyclone vulnerability and the global vanilla economy*. Altamira Press, 241-261 pp.

Chang-Seng, D. S., and M. R. Jury, 2010: Tropical cyclones in the SW Indian Ocean. Part 1: inter-annual variability and statistical prediction. *Meteorol. Atmos. Phys.*, **106,** 149-162.

Chang, I., M. L. Bentley, and J. M. Shepherd, 2014: A global climatology of extreme rainfall rates in the inner core of intense tropical cyclones. *Physical Geography*, **35,** 478-496.

Guo, Q., and C. Matyas, 2016: Comparing the spatial extent of Atlantic basin tropical cyclone wind and rain fields prior to land interaction. *Physical Geography*, **37,** 5-25.

Hill, K., and G. M. Lackmann, 2009: Influence of environmental humidity on tropical cyclone size. *Mon. Wea. Rev.*, **137,** 3294-3315.

Hoskins, B. J., and K. I. Hodges, 2005: A new perspective on Southern Hemisphere storm tracks. *J. Climate*, **18,** 4108-4129.

Jiang, H., C. Liu, and E. J. Zipser, 2011: A TRMM-based tropical cyclone cloud and precipitation feature database. *J. Appl. Meteorol. Climatol.*, **50,** 1255-1274.

Jury, M. R., B. Pathack, and B. Parker, 1999: Climatic determinants and statistical prediction of tropical cyclone days in the southwest Indian ocean. *J. Climate*, **12,** 1738-1746.

Knapp, K. R., M. C. Kruk, D. H. Levinson, H. J. Diamond, and C. J. Neumann, 2010: The International Best Track Archive for Climate Stewardship (IBTrACS): unifying tropical cyclone data. *Bull. Amer. Meteor. Soc.*, **91,** 363-376.

Lonfat, M., F. D. Marks, and S. Y. S. Chen, 2004: Precipitation distribution in tropical cyclones using the Tropical Rainfall Measuring Mission (TRMM) Microwave Imager: A global perspective. *Mon. Wea. Rev.*, **132,** 1645-1660.

Matyas, C. J., 2015: Tropical cyclone formation and motion in the Mozambique Channel. *International Journal of Climatology*, **35,** 375–390.

Matyas, C. J., 2017: Comparing the spatial patterns of rainfall and atmospheric moisture among tropical cyclones having a track similar to Hurricane Irene (2011). *Atmosphere*, **8,** 165-185.

Matyas, C. J., and J. A. Silva, 2013: Extreme weather and economic well-being in rural Mozambique. *Nat. Hazards*, **66,** 31-49.

Ord, J. K., and A. Getis, 1995: Local spatial autocorrelation statistics: distributional issues and an application. *Geogr Anal*, **27,** 286-306.

Reason, C. J. C., 2007: Tropical cyclone Dera, the unusual 2000/01 tropical cyclone season in the South West Indian Ocean and associated rainfall anomalies over Southern Africa. *Meteorol. Atmos. Phys.*, **97,** 181-188.

Reason, C. J. C., and A. Keibel, 2004: Tropical Cyclone Eline and its unusual penetration and impacts over the southern African mainland. *Wea. Forecasting*, **19,** 789-805.

Reason, C. J. C., S. Hachigonta, and R. F. Phaladi, 2005: Interannual variability in rainy season characteristics over the Limpopo region of southern Africa. *Int. J. Climatol.*, **25,** 1835-1853.

Silva, J. A., C. J. Matyas, and B. Cunguara, 2015: Regional inequality and polarization in the context of concurrent extreme weather and economic shocks. *Applied Geography*, **61,** 105-116.

Takakura, T., R. Kawamura, T. Kawano, K. Ichiyanagi, M. Tanoue, and K. Yoshimura, 2017: An estimation of water origins in the vicinity of a tropical cyclone's center and associated dynamic processes. *Climate Dynamics***,** 1-15.

Vitart, F., D. Anderson, and T. Stockdale, 2003: Seasonal forecasting of tropical cyclone landfall over Mozambique. *J. Climate*, **16,** 3932-3945.

Williams, C. J. R., D. R. Kniveton, and R. Layberry, 2007: Climatic and oceanic associations with daily rainfall extremes over southern Africa. *Int. J. Climatol.*, **27,** 93-108.

Zhou, Y., and C. J. Matyas, 2018: Spatial characteristics of rain fields associated with tropical cyclones landfalling over the western Gulf of Mexico and Caribbean Sea. *Journal of Applied Meteorology and Climatology*, **Under Review**